EurJIC
European Journal of Inorganic Chemistry

Research Article
doi.org/10.1002/ejic.202300037

Chemistry Europe
European Chemical Societies Publishing

www.eurjic.org

Isolation of Bis- and Mono-Cyclometallated Ru–IMes Complexes upon Reaction of [Ru(PPh$_3$)$_3$HCl], IMes and ZnMe$_2$

Anne-Frédérique M. Pécharman,[a] Erika M. Roberts,[a] Fedor M. Miloserdov,[a, b] Victor Varela-Izquierdo,[a, c, d] Mary F. Mahon,*[a] and Michael K. Whittlesey*[a]

Addition of an excess of ZnMe$_2$ to a mixture of [Ru(PPh$_3$)$_3$HCl] and IMes (IMes = 1,3-bis(2,4,6-trimethylphenyl)imidazolin-2-ylidene) yields the bis-cyclometallated complex, [Ru(IMes)″(PPh$_3$)$_2$] **2**, together with the mono-cyclometallated, Ru–Zn heterobimetallic complex [Ru(IMes)′(PPh$_3$)$_2$(ZnMe)] **3**. Treatment of **2** with H$_2$, PhSiH$_3$ or pinacolborane yields the previously reported complex, [Ru(IMes)′(PPh$_3$)$_2$H] **1**, the synthesis of which has been reinvestigated. Further studies of small molecule reactivity show that **1** adds H$_2$ to give [Ru(IMes)(PPh$_3$)$_2$H$_4$] **4**, whilst **2** reacts with catecholborane to give [Ru(IMes-Bcat)′(PPh$_3$)$_2$H] **5**, in which (IMes-Bcat)′ signifies a borylated NHC ligand that is singly-metallated onto Ru. Treatment of **2** with CO gives the 18-electron dicarbonyl product [Ru(IMes)″(PPh$_3$)(CO)$_2$] **6**. Compounds **1**–**3**, **5** and **6** have been structurally characterised.

Introduction

The expansive growth of transition metal N-heterocyclic carbene (TM-NHC) chemistry in the early/mid 1990–2000's[1] was fuelled by the hope that NHCs would be less susceptible to the types of degradative reactions often encountered with phosphine ligands,[2] and therefore prove beneficial for catalysis. While the value of NHCs in both homogeneous and heterogeneous environments is indisputable,[3] they have turned out to be far from innocent in terms of their properties, proving susceptible to a range of intramolecular bond cleavage reactions at both the N-substituents (e.g. C–H, C–C and C–N activation) and the imidazolin-2-ylidene, imidazolidin-2-ylidene and tetrahydropyrimidin-2-ylidene rings themselves (e.g. ring-opening and insertion).[4] C–H activation of an N-substituent is arguably the most prevalent of these reactions, being induced by metals from right across the transition metal series.[5] Although the resulting cyclometallated products prove detrimental to any subsequent useful chemistry in many cases,[6] there are examples where cyclometallation has been shown not only to enhance catalytic processes, but also to play a key role in determining selectivity.[7] As a result, considerable interest remains in accessing new cyclometallated TM-NHC complexes and undertaking studies of their reactivity.

In 2019, we reported that the reaction of [Ru(IMes)(PPh$_3$)(CO)HCl] (**I**; IMes = 1,3-bis(2,4,6-trimethylphenyl)imidazolin-2-ylidene) with ZnMe$_2$ produced the heterobimetallic Ru–Zn complex [Ru(IMes)′(PPh$_3$)(CO)(ZnMe)] (**II**; IMes′ = cyclometallated IMes) upon elimination of methane and HCl (Scheme 1).[8] Interestingly, exposure of **II** to H$_2$ resulted in addition across the Ru–Zn bond to form **III**, rather than reverse IMes metallation, as observed in many other systems.[9] These studies of **I**, together with more recent work on the reactivity of ZnMe$_2$ with the tris-phosphine precursor [Ru(PPh$_3$)$_3$HCl],[10] suggested that the addition of ZnMe$_2$ to a combination of [Ru(PPh$_3$)$_3$HCl] and IMes could lead to interesting reactivity of the NHC. Morris has previously reported that simply heating the hydride chloride precursor with just IMes gave the cyclometallated compound, [Ru(IMes)′(PPh$_3$)$_2$H] **1**.[11] Fogg showed that **1** formed under an atmosphere of argon, whereas when a blanket of N$_2$ was used, the bis-carbene dinitrogen complex, [Ru(IMes)$_2$(N$_2$)HCl], was isolated instead.[12] Others have shown that the combination of [Ru(PPh$_3$)$_3$HCl] with N-alkyl substituted NHCs yields a range of mono- and bis-NHC containing products, along with even higher coordinate Ru–NHC complexes.[11,13]

We now report that combining ZnMe$_2$, [Ru(PPh$_3$)$_3$HCl] and IMes leads to the unusual bis-cyclometallation of IMes to give

[a] Dr. A.-F. M. Pécharman, E. M. Roberts, Dr. F. M. Miloserdov, Dr. V. Varela-Izquierdo, Dr. M. F. Mahon, Prof. M. K. Whittlesey
Department of Chemistry
University of Bath
Bath BA2 3QD (UK)
E-mail: m.f.mahon@bath.ac.uk
m.k.whittlesey@bath.ac.uk
[b] Dr. F. M. Miloserdov
Present Address: Laboratory of Organic Chemistry
Wageningen University
Stippeneng 4, Wageningen 6708 WE (The Netherlands)
[c] Dr. V. Varela-Izquierdo
Instituto de Síntesis Química y Catálisis Homogénea (ISQCH)
CSIC-Universidad de Zaragoza
Pedro Cerbuna 12, 50009-Zaragoza (Spain)
[d] Dr. V. Varela-Izquierdo
Present Address: LPCNO, Laboratoire de Physique et Chimie de Nano-Objets, UMR, 5215 INSA-CNRS-UPS, Institut National des Sciences Appliquées
135 avenue de Rangueil, 31077 Toulouse (France)

Supporting information for this article is available on the WWW under https://doi.org/10.1002/ejic.202300037

Part of the "NHC-Ligands in Organometallic Chemistry and Catalysis" Special Collection.

Research Article
doi.org/10.1002/ejic.202300037

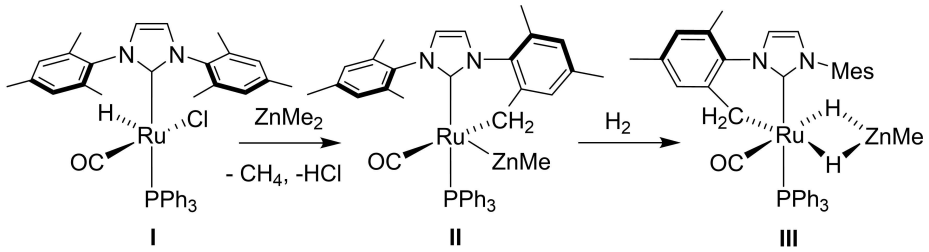

Scheme 1. Preparation of [Ru(IMes)′(PPh$_3$)(CO)(ZnMe)] **II** and reaction with H_2.

[Ru(IMes)″(PPh$_3$)$_2$] **2**. The reaction also affords [Ru(IMes)′(PPh$_3$)$_2$(ZnMe)] **3**, a heterobimetallic analogue of **1** (Scheme 2). Complex **2** undergoes hydrogenation of one of the metallated N-Mes substituents in the presence of H_2, $PhSiH_3$ and HBpin to give **1**, which itself can be further hydrogenated with H_2. In contrast to the reaction with pinacolborane, HBcat reacts with **2** to generate [Ru(IMes-Bcat)′(PPh$_3$)$_2$H] through a B–C bond coupling reaction.

Results and Discussion

ZnMe$_2$ promoted cyclometallation of [Ru(PPh$_3$)$_3$HCl]/IMes

We are unaware of any reported study of the reactivity of [Ru(PPh$_3$)$_3$HCl] towards IMes at room temperature. Using NMR monitoring in THF solution, we found that a 1:1 molar ratio of [Ru(PPh$_3$)$_3$HCl]:IMes rapidly generated two new hydride containing species with resonances at $\delta = -16.9$ ppm (singlet) and $\delta = -20.8$ ppm (triplet, $J_{H,P} = 31.3$ Hz). Some of the ruthenium precursor remained unconsumed even after a week. Increasing the number of equivalents of IMes to 3 resulted in the almost complete consumption of [Ru(PPh$_3$)$_3$HCl], an increase in the magnitude of the resonance at $\delta = -16.9$ ppm relative to that at $\delta = -20.8$ ppm, and the formation of a small amount of a third new hydride containing species, which appeared as a doublet ($J_{H,P} = 42.2$ Hz) at $\delta = -30.4$ ppm (Figure S1). Comparison of the chemical shifts and coupling constants to those of the previously reported mono- and bis-N-cyclohexyl derivatives [Ru(ICy)(PPh$_3$)$_2$HCl] and [Ru(ICy)$_2$(PPh$_3$)HCl][13a] (ICy = 1,3-dicyclohexylimidazolin-2-ylidene) led us to assign the signals at $\delta = -20.8$ ppm and $\delta = -30.4$ ppm to [Ru(IMes)(PPh$_3$)$_2$HCl] and [Ru(IMes)$_2$(PPh$_3$)HCl] respectively. The species responsible for the singlet hydride resonance is unclear. It clearly cannot be phosphorus containing. A 14-electron bis-carbene species such as [Ru(IMes)$_2$HCl] seems unlikely on the basis of the very high coordinative unsaturation,[14] as well as the presumed paramagnetism by analogy to [Ru(IMes)$_2$Cl$_2$].[7e] The tris-carbene complex [Ru(IMes)$_3$HCl] also seems unlikely on the grounds of sterics, but in the absence of any simple mononuclear alternative,[15] must be considered plausible (Scheme 2). Varying the solvent failed to simplify the mixture of products,[16] in contrast to our previous findings with ICy.[13a]

Given the formation of a mixture of Ru–H containing products irrespective of the number of equivalents of IMes present, we chose to react [Ru(PPh$_3$)$_3$HCl] with an excess of IMes (3 eq), prior to addition of an excess of ZnMe$_2$ (5 eq), to ensure consumption of the ruthenium phosphine precursor and prevent it reacting with ZnMe$_2$.[10] Under these conditions, the formation of two ruthenium containing products, the doubly cyclometallated IMes complex, [Ru(IMes)″(PPh$_3$)$_2$] **2**, and [Ru(IMes)′(PPh$_3$)$_2$(ZnMe)] **3** (Scheme 3) were apparent by ^{31}P{^{1}H} NMR spectroscopy within minutes (Figure S2). The formation of some [Zn(IMes)Me$_2$] through combination of the excess ZnMe$_2$ and excess IMes was also apparent by ^{1}H NMR spectroscopy.[17]

Crystallisation of a crude reaction mixture by slow evaporation from Et$_2$O afforded, in the first instance, dark red crystals of **2**. Only poor yields of material (10–32%) proved isolable as crystallisation for longer time co-deposited purple-red crystals of **3**, along with colourless [Zn(IMes)Me$_2$]. Single crystal picking provided **3** suitable for an X-ray structural determination, but we were unable to isolate enough pure sample for elemental analysis.

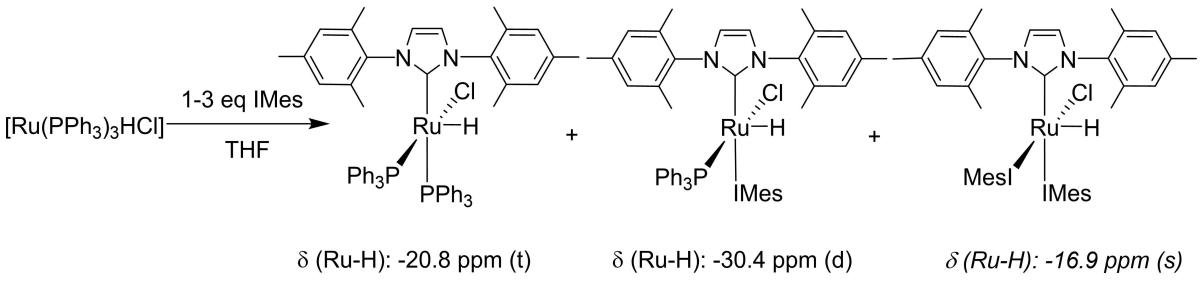

Scheme 2. Proposed products from the room temperature reaction of [Ru(PPh$_3$)$_3$HCl] and IMes. The italicised characterisation data for [Ru(IMes)$_3$HCl] are intended to emphasise the uncertainty surrounding this particular assignment.

Research Article
doi.org/10.1002/ejic.202300037

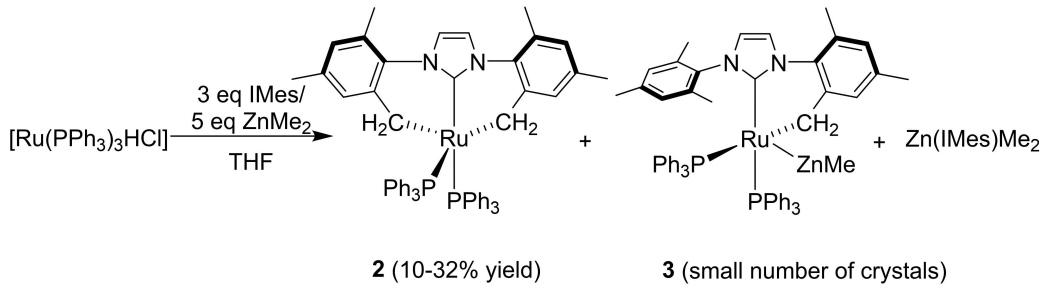

Scheme 3. Formation of **2** and **3** from reaction of $ZnMe_2$ with $[Ru(PPh_3)_3HCl]$ and IMes.

The X-ray crystal structures of **2** and **3** are shown in Figure 1, with key structural metrics given in Table 1. Complex **2** adopts a 5-coordinate, pseudo square pyramidal structure in which the ruthenium centre is coordinated to a tridentate IMes ligand resulting from the metalation of an *ortho*–CH_3 group on each of the N–Mes substituents. Metal complexes featuring a doubly metallated NHC ligand are rare, with only a few examples known for Ir and Ru.[18,19] One Ru–CH_2 group occupies the apical position trans to a vacant site and, as a result, exhibited a much shorter Ru–C distance (2.1051(17) Å) than that situated pseudo-trans (∠C2-Ru1-P2 = 154.995°) to one of the two PPh_3 ligands (2.1708(18) Å). The tridentate coordination motif impacted significantly on the Ru–C_{IMes} distance, which at 2.0319(17) Å, was shorter than that in mono-metallated **3** (2.066(3) Å). The latter also featured a square pyramidal structure, with an apical ZnMe ligand opposite the vacant site. The Ru–Zn bond length (2.3591(4) Å) was well-within the sum of the covalent radii (Ru: 1.46 Å; Zn: 1.22 Å),[20] although short in comparison to the

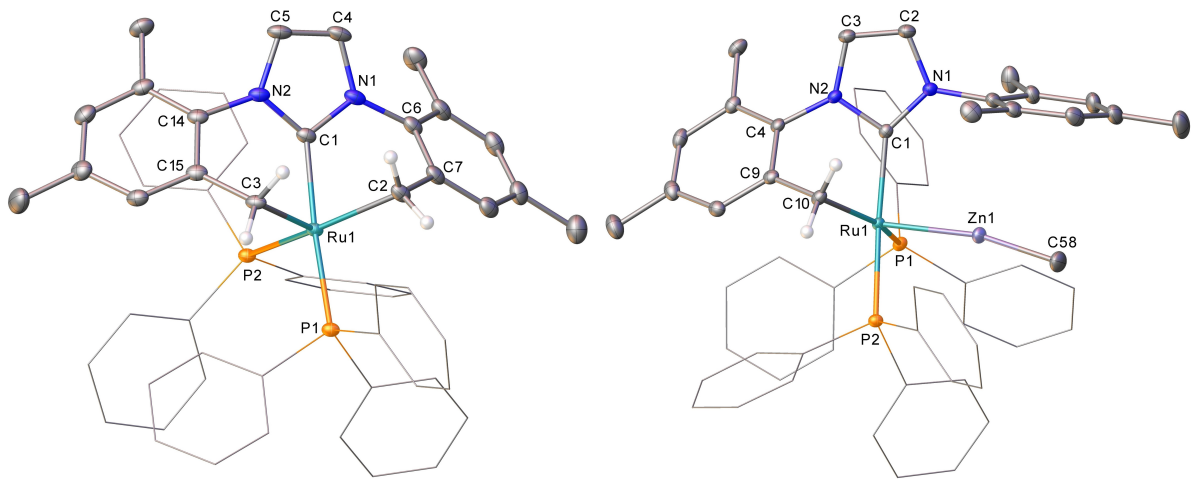

Figure 1. Molecular structures of (left) [Ru(IMes)"$(PPh_3)_2$] **2** and (right) [Ru(IMes)'$(PPh_3)_2$(ZnMe)] **3**. In both cases, ellipsoids are represented at 30% probability and phosphine phenyl groups are shown in wireframe view. For clarity, the hydrogen atoms in **2** (except those attached to C2 and C3), together with the solvent and hydrogen atoms in **3** (except those attached to C10), have been omitted.

Table 1. Selected bond lengths (Å) and angles (°) in the Ru(IMes)' and Ru(IMes)'' complexes **1**–**3**, **5** and **6**.

	1	**2**	**3**	**5**	**6**
Ru–C_{NHC}	2.0659(17)	2.0319(17)	2.066(3)	2.077(3)	2.0739(19)
Ru–P	2.3034(4) 2.3027(4)	2.3510(4) 2.3393(4)	2.3203(7) 2.2975(7)	2.3196(9) 2.2878(9)	2.3778(5)
Ru–CH_2	2.1639(16)	2.1708(18) 2.1051(17)	2.179(3)	2.216(3)	2.2083(19) 2.2055(19)
Ru–Zn	–	–	2.3591(4)	–	–
Ru–*C*O	–	–	–	–	1.915(2)
C_{NHC}–Ru–*P*	159.73(5) 91.70(5)	165.90(5) 91.70(5)	159.89(8) 99.11(8)	162.05(9) 96.78(9)	161.68(5)
HX*C*–Ru–*P*	(*X*=*H*) 161.65(5) 86.06(5)	(*X*=*H*) 154.99(5) 91.65(5) 106.00(5) 91.02(5)	(*X*=*H*) 153.55(8) 87.85(8)	(*X*=*Bcat*) 159.31(9) 86.27(9)	(*X*=*H*) 91.52(5) 87.04(5)

Research Article
doi.org/10.1002/ejic.202300037

Ru–Zn distances observed in related compounds previously reported by our group.[21]

The $^{31}P\{^1H\}$ NMR spectrum of **2** showed two doublets at $\delta =$ 49.8 ppm and $\delta = 34.8$ ppm ($^2J_{P,P} = 16$ Hz), whilst the ^1H NMR spectrum displayed a doublet at $\delta = 3.16$ ppm and doublet of doublets at $\delta = 2.54$ ppm (each of relative integral 2) diagnostic of the diastereotopic Ru–CH_2 protons (Figures S3 and S4). For **3**, the $^{31}P\{^1H\}$ NMR spectrum comprised of an AB resonance at ca. $\delta = 56$ ppm, and the ^1H NMR spectrum displayed a broad multiplet and doublet of doublet of doublets (at $\delta = 3.83$ ppm and $\delta = 2.32$ ppm respectively, each of relative integral 1) for the Ru-bound methylene group (Figures S6 and S7).

Complex **2** proved to be moderately robust in solution, with only small amounts of new signals apparent by NMR spectroscopy after heating for days at 40 °C in C_6D_6. These signals increased in intensity upon raising the temperature to 60 °C, and there was also now ^{31}P NMR evidence for some H/D exchange with the solvent into the PPh_3 ligands of **2** (Figure S11).

Reactivity of 2 with H_2

Addition of 1 atm H_2 readily converted **2** into two new hydride containing species, which appeared in the ^1H NMR spectrum (in $C_6D_5CD_3$ at 255 K) as a broad singlet at $\delta = -7.16$ ppm and a doublet of doublets at $\delta = -28.3$ ppm, in a relative ratio of ca. 1.3:1 (Figure S12). Two $^{31}P\{^1H\}$ NMR doublets at $\delta = 58.3$ ppm and $\delta = 57.7$ ppm accompanied the lower frequency hydride signal, consistent with this species being $[Ru(IMes)'(PPh_3)_2H]$ **1**[11] formed upon hydrogenation of one of the cyclometallated N–Mes groups in **2**. The second, broad hydride containing product was assigned to $[Ru(IMes)(PPh_3)_2H_4]$ **4** (see below, Scheme 4) resulting from a second hydrogenation step. Cooling to 212 K failed to resolve any coupling on the hydride signal of **4**, and indeed, **1** also now broadened to a singlet.[22] Notable was the change in relative ratio to ca. 3.8:1, consistent with **1** being an intermediate en-route to **4**. Warming increased the ratio of **4**:**1** further (ca. 6.6:1 at 318 K); at all temperatures, the hydride resonance for **4** remained a singlet.

We attempted to access **4** alone by hydrogenation of **1**. At first this proved problematic as our efforts to reproduce the literature synthesis of **1** (heating $[Ru(PPh_3)_3HCl]$ with 2 equiv. IMes in THF for 12 h at 66 °C)[11] gave only trace amounts of the desired product. $^{31}P\{^1H\}$ NMR monitoring revealed that conversion to **1** necessitated longer times, with optimal conversion found after 72 h (Figure S13).[23] This allowed isolation of **1** as a red microcrystalline solid in 40% yield (Figures S14–S16).[24] An X-ray crystal structure (Figure 2 and Table 1) showed the compound to be isostructural with the SIMes analogue,[11] even down to the acute Ru–CH_2–$C_6Me_2H_2$ angle (91.47(11)° vs. 89.6°).[25]

Subjecting a C_6D_6 solution of **1** to 1 atm H_2 led to a rapid colour change from red to colourless, with concomitant formation of the broad hydride resonance for **4** (Figure S17). Integration confirmed a value of 4 H relative to the backbone NC*H* and mesityl CH_3 resonances. Given both the temperature invariant broadness of the signal and the short T_1 value of 37 ms determined at room temperature (400 MHz), **4** is best formulated as the fluxional dihydrogen dihydride complex shown in Scheme 4. Attempts to isolate **4** for structural verification were thwarted by the rapid loss of H_2 and reversion to **1** upon removal of the H_2 atmosphere. Despite this, our assignment is supported by the presence of analogous $[RuL_3(\eta^2\text{–}H_2)H_2]$ structures in the literature.[26]

Reactivity of 2 with Si–H and B–H bonds

Prompted by the facile reactions of **1** and **2** with H_2, we then turned our attention to silanes and boranes (Scheme 5). $PhSiH_3$ underwent rapid dehydrogenation (< 5 min, room temperature) by **2** to give **1** as the only detectable ruthenium containing product by ^1H and ^{31}P NMR spectroscopy (Figure S19). The fate of Si was unclear. Et_3SiH failed to give the same reaction, even upon warming to 40 °C, although H/D exchange with C_6D_6 was now observed, both at a lower temperature and to a greater extent than found when **2** was simply heated in C_6D_6 in the absence of any silane (Figures S20–S22).

$[Ru(IMes)'(PPh_3)_2H]$ **1** was also the only Ru-containing product formed upon treatment of **2** with 1 equiv. pinacolborane (HBpin). However, addition of a second equivalent of HBpin led to the depletion of **1** (there was no reaction of **1** with excess $PhSiH_3$) and the appearance in the ^1H NMR spectrum of multiple new sharp hydride resonances between ca. $\delta = -26$ ppm and $\delta = -29$ ppm, as well as new, broad and overlapping hydride resonances at ca. $\delta = -7$ ppm. When a third equivalent of HBpin was added, the higher frequency signals were dominant (Fig-

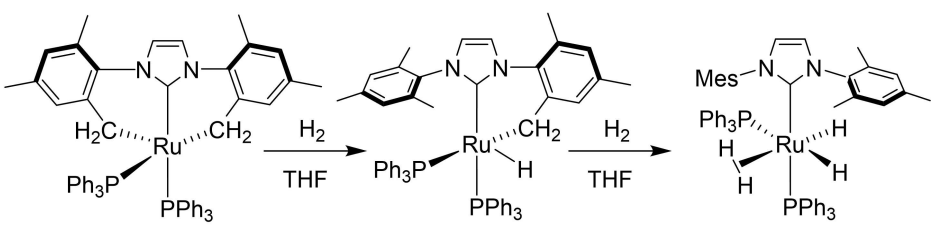

2 **1** **4**

Scheme 4. Formation of $[Ru(IMes)(PPh_3)_2H_4]$ **4** from addition of H_2 to **1** and **2**.

Research Article
doi.org/10.1002/ejic.202300037

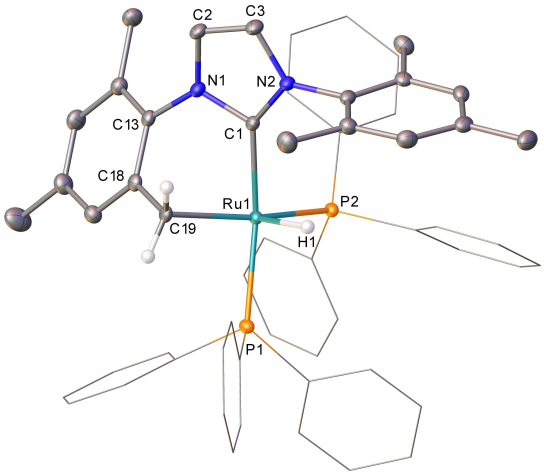

Figure 2. Molecular structure of [Ru(IMes)′(PPh_3)$_2$H] **1** with ellipsoids represented at 30% probability. Hydrogen atoms (those attached to C19 and the hydride ligand excepted) have been omitted and phosphine phenyl groups are shown in wireframe view, for clarity.

ure S23). The similarity (both in terms of broadness and chemical shift) to the Ru–H/H_2 signals of **4** suggests that they may arise from σ-borane hydride containing products, although as for **4**, unequivocal, structural verification was thwarted by decomposition following removal of the HBpin.

Very different behaviour was observed with catecholborane (HBcat). ^{1}H NMR spectra recorded within a few minutes of combining **2** and 1 equiv. of the borane in C_6D_6 showed not only formation of **1**, but also a new hydride containing species **5**, which exhibited an extremely similar Ru–H chemical shift ($\delta = -27.29$ ppm) and coupling parameters (dd, $^2J_{P,P} = 31$ and 25 Hz) to those of **1**. Complete conversion to **5** took place over 2 h (Figure S24), allowing the product to be isolated and characterised using a combination of X-ray and NMR measurements (Figures S25–S28) as [Ru(IMes–Bcat)′(PPh_3)$_2$H], where IMes–Bcat′ denotes the boryl-substituted cyclometallated IMes ligand shown in Scheme 5.

Borylation of the methylene arm attached to Ru is shown unequivocally in the X-ray structure in Figure 3. The Ru–*C*H-(Bcat) distance (2.216(3) Å) was somewhat longer than the Ru–CH_2 distance in **1** (2.1639(16) Å), most likely as a result of sterics. C–B bond coupling at a metallated NHC has been observed previously at both Ir(III)[18a] and Pt(II) centres,[27]

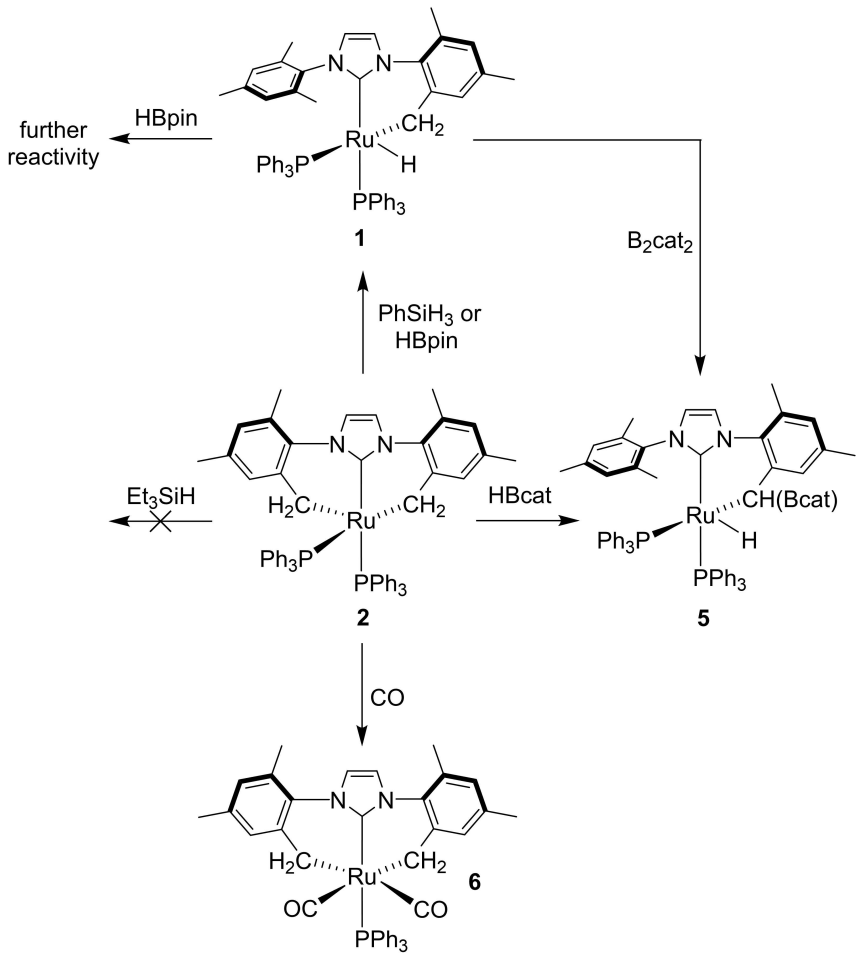

Scheme 5. Summary of the reactivity of **2** with E–H bonds and CO.

Research Article
doi.org/10.1002/ejic.202300037

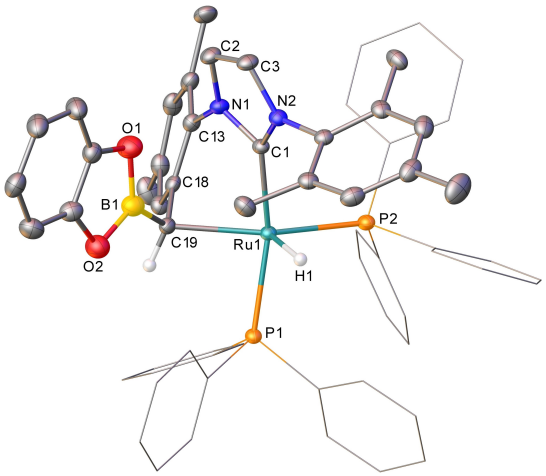

Figure 3. Molecular structure of [Ru(IMes–Bcat)′$(PPh_3)_2$H] **5** with ellipsoids represented at 30% probability. Solvent and hydrogen atoms (except for the hydride ligand and that attached to C19) have been omitted for clarity. The phosphine phenyl groups are shown in wireframe view, again, for clarity.

although in these examples, the borylated arm is no longer coordinated to the metal.[28,29] Tilley has reported the formation of a borylated IXylyl ligand (IXylyl = 1,3-bis(2,6-dimethyphenyl)imidazolin-2-ylidene) upon treatment of [Cp*Ru-(IXylyl)′(N_2)] with $B(C_6F_5)_3$ (Scheme 6). Although this also stays non-metallated, it does exhibits stabilising *ipso*-C[30] and C–H agostic interactions with the Ru centre.[18d]

Scheme 7 outlines pathways that could account for the appearance of both **5** and **1** and, ultimately, complete conversion to the former. In pathway (a), direct formation of **5** could proceed upon displacement of a PPh_3 ligand by borane and a σ-CAM step,[31] which when followed by subsequent reductive elimination of the resulting ruthenium hydride and remaining –CH_2(aryl) arm, affords a highly unsaturated Ru(0) intermediate. Insertion of this species into a C–H bond of the –CH_2(Bcat) arm would yield **5**. To account for the formation of **1** alongside **5** in early stages of the reaction (Figure S24), an additional pathway (b), involving H- rather than Bcat-transfer onto the metallated NHC[27a] could occur, to give a Ru–boryl intermediate. Coordination of HBcat, followed by elimination of B_2cat_2 and re-coordination of PPh_3 affords **1**. Subsequent transformation of **1** to **5** could proceed by B–B activation of the diborane and, indeed, this is what was observed when **1** was reacted with 1 equiv. B_2cat_2 at room temperature (Scheme 5, Figure S29).

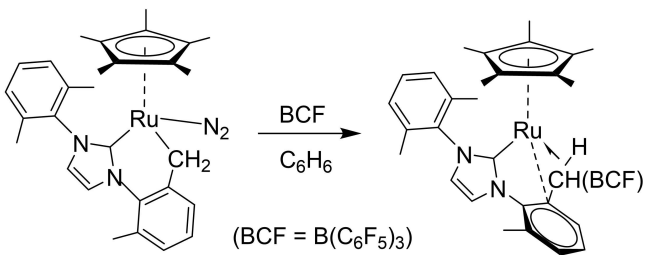

Scheme 6. Reported C–B bond formation at a [Ru(IXylyl)′] ligand.[18d]

Coordinative saturation of 2 by CO

The deep red/orange colours exhibited by compounds **1**, **2**, **3** and **5** are consistent with their coordinative unsaturation. Upon exposure of **2** to CO (1 atm), an instantaneous colour change from red to colourless was observed resulting from the formation of the 18-electron dicarbonyl complex [Ru-(IMes)″$(PPh_3)(CO)_2$] (**6**, Scheme 5). Spectroscopically, the reaction was accompanied by the appearance of a new singlet resonance at $\delta = 46$ ppm in the $^{31}P\{^1H\}$ NMR spectrum (Figure S31), together with a resonance for free PPh_3, consistent with the substitution of one of phosphine ligands by CO. The X-ray crystal structure of **6** (Figure 4) confirmed the retention of the doubly metallated IMes ligand. The methylene groups were now trans to CO, and as a result, exhibited elongated Ru–CH_2 distances (2.2055(19) and 2.2083(19) Å) relative to those in **2**.

Conclusions

The combination of [Ru$(PPh_3)_3$HCl] with excess IMes and $ZnMe_2$ affords a mixture of the doubly cyclometallated IMes complex [Ru(IMes)″$(PPh_3)_2$] **2** and the heterobimetallic mono-metallated IMes species [Ru(IMes)′$(PPh_3)_2$(ZnMe)] **3**. The generation of non-Zn containing **2** contrasts with our previous observation on adding $ZnMe_2$ to both [Ru$(PPh_3)_3$HCl] and [Ru-(IMes)(PPh_3)(CO)HCl], which yield only Ru–Zn heterobimetallic products.[8,10]

Complex **2** represents a rare example of a doubly cyclometallated NHC–TM product. One of the two metallated arms can be readily hydrogenated by H_2 to form [Ru(IMes)′$(PPh_3)_2$H] **1**, previously reported by Morris, and ultimately a product we assign as [Ru(IMes)$(PPh_3)_2H_4$] **4**. Hydrogenation reactions are

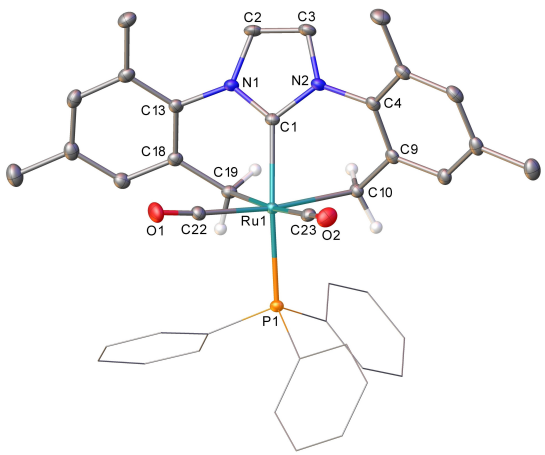

Figure 4. Molecular structure of [Ru(IMes)″$(PPh_3)(CO)_2$] **6** with ellipsoids represented at 30% probability. Hydrogen atoms (those attached to C10 and C19 excepted) have been omitted and phosphine phenyl groups are shown in wireframe view, for clarity.

Research Article
doi.org/10.1002/ejic.202300037

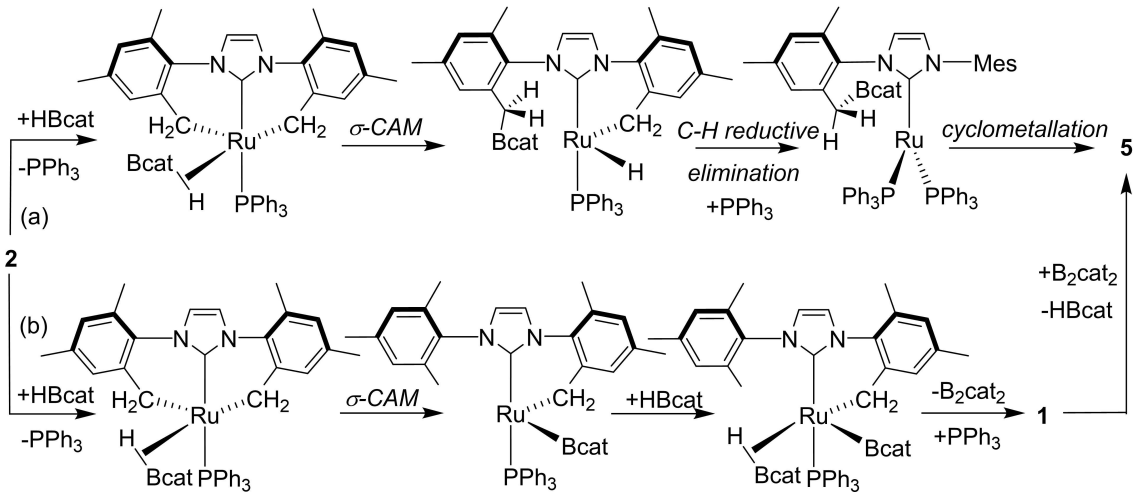

Scheme 7. Possible pathways (a and b) to formation of [Ru(IMes-Bcat)′(PPh$_3$)$_2$H] **5** from the reaction of **2** and HBcat.

also found with both PhSiH$_3$ and HBpin. Interestingly, Sola and co-workers found a similar preference for the dehydrogenation of silanes and boranes and hydrogenation of the {TM(IMes)′′} moiety during their studies of [Ir(IMes)′′(P^{i}Pr$_3$)(MeCN)$_2$][PF$_6$].[18a]

In contrast to the formation of **1** from **2** and HBpin, changing the borane to HBcat gave [Ru(IMes-Bcat)′(PPh$_3$)$_2$H] **5**, which contains a boryl functionalised (IMes) ligand. We believe that the different reactivity of **2** towards the two boranes supports the assertion in the introduction to this manuscript that cyclometallated TM–NHC complexes still remain of considerable interest.

Experimental Section

General Considerations: All manipulations were carried out under argon using standard Schlenk, high vacuum and glovebox techniques using dry and degassed solvents. C$_6$D$_6$, C$_6$D$_5$CD$_3$ and [D8]THF were vacuum transferred from potassium. NMR spectra were recorded at 298 K (unless otherwise stated) on Bruker Avance 400 and 500 MHz NMR spectrometers and referenced as follows: C$_6$D$_6$ (^{1}H, δ = 7.15 ppm; ^{13}C, δ = 128.0 ppm), C$_6$D$_5$CD$_3$ (^{1}H, δ = 2.09 ppm) and [D8]THF (^{1}H, δ = 3.58 ppm; ^{13}C, δ = 67.6 ppm). ^{31}P and ^{11}B spectra were referenced externally to 85% H$_3$PO$_4$ (δ = 0.0 ppm) and BF$_3$·OEt$_2$ (δ = 0.0 ppm) respectively. IR spectra were recorded on a Bruker ALPHA ATR-IR spectrometer. Elemental analyses were performed by Elemental Microanalysis Ltd, Okehampton, Devon, U.K. [Ru(PPh$_3$)$_3$HCl]·toluene and IMes were prepared according to the literature.[32,33]

[Ru(IMes)′′(PPh$_3$)$_2$] 2 and [Ru(IMes)′(PPh$_3$)$_2$(ZnMe)] 3: A THF (3 mL) solution of [Ru(PPh$_3$)$_3$HCl]·0.8toluene (100 mg, 0.10 mmol) and IMes (91 mg, 0.30 mmol) was stirred for 18 h at room temperature before ZnMe$_2$ (410 μL of 1.2 M in toluene, 0.49 mmol) was added and the solution stirred for an additional day. Removal of the volatiles afforded a red oil, which was dissolved in a minimal amount of Et$_2$O, filtered and the filtrate then slowly evaporated in a glovebox at room temperature to give dark red crystals of **2** overnight. These were isolated, washed with 1 mL Et$_2$O and dried under vacuum. Yields varied between 10–30 mg (10–32% yield), depending on crystallisation time; ca. 12 h afforded lower yields, but of analytically pure compound. Efforts to increase the yield of **2** by evaporating for longer times resulted instead in co-crystallisation with purple-red crystals of **3**, together with colourless material, which NMR spectroscopy showed to be a mixture of [Zn(IMes)Me$_2$] and PPh$_3$. As a result, not only were we unable to increase the yield of **2** above ca. 30%, but were unable to isolate analytically pure **3**. Compound **2**. ^{1}H NMR (500 MHz, C$_6$D$_6$, 298 K): δ = 7.36–7.28 (m, 6H, Ar), 7.00–6.92 (m, 9H, Ar), 6.85–6.79 (m, 3H, Ar), 6.77–6.71 (m, 8H, Ar), 6.66 (s, 2H, Ar), 6.60 (s, 2H, Ar), 6.51 (t, $J_{H,H}$ = 8.0 Hz, 6H, Ar), 3.16 (br d, $^2J_{H,H}$ = 8.2 Hz, 2H, RuC*H*H), 2.54 (dd, J = 12.5 Hz, ^2J = 8.2 Hz, 2H, RuCH*H*), 2.25 (s, 6H, C$_6$*Me*$_2$H$_3$), 1.87 (s, 6H, C$_6$*Me*$_2$H$_3$) ppm. ^{31}P{^{1}H} NMR (202 MHz, C$_6$D$_6$, 298 K): δ = 49.8 (d, $^2J_{P\text{-}P}$ = 16 Hz), 34.8 (d, $^2J_{P\text{-}P}$ = 16 Hz) ppm. ^{13}C{^{1}H} DEPTQ NMR (101 MHz, [D8]THF, 298 K): δ = 205.9 (dd, $^2J_{C,P}$ = 92 Hz, $^2J_{C,P}$ = 12 Hz, Ru–*C*$_{NHC}$), 148.8 (s, *C*$_{quat}$), 141.2 (d, $^1J_{C,P}$ = 23 Hz, P*C*$_{quat}$), 138.7 (d, $^1J_{C,P}$ = 28 Hz, *C*H$_{Ar}$), 136.3 (s, *C*$_{quat}$), 130.5 (s, *C*$_{quat}$), 128.7 (s, *C*H$_{Ar}$), 128.2 (s, *C*H$_{Ar}$), 128.1 (s, *C*H$_{Ar}$), 128.0 (s, *C*H$_{Ar}$), 127.0 (s, *C*H$_{Ar}$), 127.9 (s, *C*H$_{Ar}$), 124.4 (s, *C*H$_{Ar}$), 119.9 (d, $J_{C,P}$ = 2 Hz, NC*H*=NCH), 21.4 (s, C$_6$*Me*$_2$H$_2$), 19.6 (s, C$_6$*Me*$_2$H$_2$), 14.3 (dd, $^2J_{C,P}$ = 24 Hz, $^2J_{C,P}$ = 7 Hz, Ru–*C*H$_2$) ppm. Elemental analysis calcd (%) for C$_{57}$H$_{52}$N$_2$P$_2$Ru [928.03]: C, 73.77; H, 5.65; N, 3.02. Found: C, 73.42; H, 5.50; N, 2.95. Compound **3**. ^{1}H NMR (400 MHz, C$_6$D$_6$, 298 K): δ = 7.41 (m, 5H, Ar), 7.28-7.22 (m, 6H, Ar), 7.00–6.86 (m, 20H, Ar), 6.75 (br s, 1H, Ar), 6.69 (br, 1H, Ar) 6.52 (d, $^3J_{H,H}$ = 2.0 Hz, 1H, NCH=C*H*N), 6.22 (d, $^3J_{H,H}$ = 2.0 Hz, 1H, NC*H*=CHN), 5.24 (br s, 1H, Ar), 3.83 (br m, 1H, RuC*H*H), 2.59 (s, 3H, C$_6$*Me*H$_3$), 2.32 (ddd, J = 15.8 Hz, J = 7.2 Hz, J = 3.0 Hz, 1H, RuCH*H*), 2.22 (s, 6H, C$_6$*Me*H$_3$), 2.19 (s, 6H, C$_6$*Me*H$_3$), 2.09 (s, 3H, C$_6$*Me*H$_3$), 1.24 (s, 3H, C$_6$*Me*H$_3$), −0.83 (s, 3H, Zn*Me*) ppm. ^{31}P{^{1}H} NMR (202 MHz, C$_6$D$_6$, 298 K): δ = 56.3 (AB, ν$_A$ = 56.4, ν$_B$ = 56.3, $J_{A,B}$ = 18 Hz) ppm. ^{13}C{^{1}H} DEPTQ NMR (101 MHz, [D8]THF, 298 K): δ = 206.3 (dd, $^2J_{C,P}$ = 82 Hz, $^2J_{C,P}$ = 9 Hz, Ru–*C*$_{NHC}$), 144.0 (d, $^2J_{C,P}$ = 29 Hz, P*C*$_{quat}$), 141.8 (d, $^2J_{C,P}$ = 32 Hz, P*C*$_{quat}$), 140.1 (s, *C*$_{quat}$), 138.4 (s, *C*$_{quat}$), 138.2 (s, *C*$_{quat}$), 137.5 (s, *C*$_{quat}$), 137.3 (s, *C*q$_{uat}$), 135.5 (br d, $J_{C,P}$ = 9 Hz, P*C*H$_{Ar}$), 133.9 (d, $J_{C,P}$ = 12 Hz, PC*H*$_{Ar}$), 131.8 (s, *C*H$_{Ar}$), 131.6 (br s, *C*H$_{Ar}$), 130.6 (s, *C*H$_{Ar}$), 128.3 (s, *C*H$_{Ar}$), 128.0 (d, $J_{C,P}$ = 8 Hz, PC*H*$_{Ar}$), 127.7 (s, *C*H$_{Ar}$), 127.6 (s, *C*H$_{Ar}$), 125.8 (br s, NC*H*=NCH), 121.7 (br s, NCH=NC*H*), 31.1 (dd, $^2J_{C,P}$ = 31 Hz, $^2J_{C,P}$ = 13 Hz, Ru–*C*H$_2$), 21.9 (s, C$_6$*Me*H$_2$), 21.4 (s, C$_6$*Me*H$_2$), 19.3 (s, C$_6$*Me*H$_2$), 18.8 (s, C$_6$*Me*H$_2$), 17.5 (s, C$_6$*Me*H$_2$), −2.8 (br, Zn*Me*) ppm.

[Ru(IMes)′(PPh$_3$)$_2$H] 1: A THF (3 mL) suspension of [Ru(PPh$_3$)$_3$HCl]·0.8toluene (400 mg, 0.39 mmol) and IMes (299 mg, 0.98 mmol) was heated in a J. Youngs resealable ampoule at 70 °C. Periodic removal of sample and monitoring by NMR spectroscopy showed that conversion to **1** was complete after 3 days. The

volatiles were removed under reduced pressure and the solid extracted in a minimum amount of Et_2O (ca. 5 mL). Slow evaporation of the Et_2O solution in the glovebox afforded an initial set of red crystals (40 mg) of [Ru(IMes)"$(PPh_3)_2$] **2**. These were removed and the filtrate evaporated further to give red crystals of **1** (160 mg, 40%). The spectroscopic data are in good agreement with those reported by Morris.[11] ^{1}H NMR (500 MHz, C_6D_6, 298 K): δ = 7.25–7.18 (m, 5H, Ar),* 7.06–6.81 (m, 17H, Ar), 6.78 (br s, 1H, Ar), 6.65 (d, $^3J_{H,H}$ = 2 Hz, 1H, Ar), 6.51 (br s, 1H, Ar), 6.22 (d, $^3J_{H,H}$ = 2 Hz, 1H, Ar), 5.10 (br s, 1H, Ar), 3.83 (m, 1H, RuC*H*H), 2.85 (s, 3H, $C_6Me_2H_3$), 2.44 (s, 3H, $C_6Me_2H_3$), 2.33 (s, 3H, $C_6Me_2H_3$), 2.21 (m, 1H, RuCH*H*), 1.98 (s, 3H, $C_6Me_2H_3$), 0.85 (s, 3H, $C_6Me_2H_3$), −28.04 (dd, $^2J_{H,P}$ = 27.9 Hz, $^2J_{H,P}$ = 25.0 Hz, 1H, Ru–*H*) ppm. *The remaining aromatic protons are obscured by the C_6D_5H resonance. ^{31}P{^{1}H} NMR (162 MHz, C_6D_6, 298 K): δ = 58.6 (AB, ν_A = 58.8, ν_B = 58.3, $J_{A,B}$ = 14 Hz) ppm. Elemental analysis calcd (%) for $C_{57}H_{54}N_2P_2Ru$ [930.05]: C, 73.61; H, 5.85; N, 3.01. Found: C, 73.77; H, 5.75; N, 3.01.

[Ru(IMes)$(PPh_3)_2(\eta^2$–$H_2)H_2$] **4**: 1 atm H_2 was added to a C_6D_6 (0.5 mL) solution of **1** (10 mg, 0.02 mmol) in a J. Young's releasable NMR tube. A rapid colour change from red to colourless occurred within 5 min, which by NMR spectroscopy, was concomitant with formation of **4**. The product was characterised by ^{1}H and ^{31}P NMR spectroscopy, but could not be isolated, as removal of the H_2 atmosphere led to reformation of **1**. ^{1}H NMR (400 MHz, C_6D_6, 298 K): δ = 7.34–7.27 (m, 1H, Ar), 6.96–6.85 (m, 23H, Ar), 6.30 (s, 2H, NC*H*=C*H*N), 2.29 (s, 6H, $C_6Me_3H_2$), 2.00 (s, 6H, $C_6Me_3H_2$), −6.82 (br s, 4H, Ru*H*) ppm. ^{31}P{^{1}H} NMR (202 MHz, C_6D_6, 298 K): δ = 57.5 (s) ppm.

[Ru(IMes-Bcat)'$(PPh_3)_2$H] **5**: Hbcat (2.1 μL, 0.018 mmol) was added to a C_6D_6 solution (0.5 mL) of **2** (20 mg, 0.02 mmol) in a J. Youngs resealable NMR tube and the reaction monitored by NMR spectroscopy over 1 h. The solution was concentrated and layered with hexane to give 11 mg **5** as red-purple crystals (57% yield). ^{1}H NMR (C_6D_6, 400 MHz, 298 K): δ = 7.29 (t, *J* = 8.5 Hz, 6H, Ar), 7.10–6.99 (m, 10H, Ar), 6.98–6.83 (m, 19H, Ar), 6.81 (br s, 1H, Ar), 6.38 (br s, 1H, NCH=C*H*N), 6.06 (d, $^3J_{H,H}$ = 1.6 Hz, NC*H*=CHN), 5.14 (br s, 1H, Ar), 2.84 (dd, *J* = 11.7 Hz, *J* = 5.1 Hz, 1H, Ru–*CH*(Bcat)), 2.52 (s, 3H, Mes), 2.39 (s, 3H, Mes), 2.18 (s, 3H, Mes), 2.03 (s, 3H, Mes), 0.64 (s, 3H, Mes), −27.29 (dd, $^2J_{H,H}$ = 31.4 Hz, $^2J_{H,H}$ = 25.0 Hz, 1H, Ru–*H*) ppm. *The remaining aromatic proton is obscured by the C_6D_5H resonance. ^{31}P{^{1}H} NMR (162 MHz, C_6D_6, 298 K): δ = 65.2 (d, $^2J_{P,P}$ = 16 Hz), 52.8 (d, $^2J_{P,P}$ = 16 Hz) ppm. ^{13}C{^{1}H} DEPTQ NMR (101 MHz, C_6D_6, 298 K): δ = 198.8 (dd, $^2J_{C,P}$ = 89 Hz, $^2J_{C,P}$ = 12 Hz, Ru–C_{NHC}), 150.3 (s, C_{quat}), 139.9 (d, $^2J_{C,P}$ = 31 Hz, C_{quat}), 138.1 (s, C_{quat}), 137.6 (s, C_{quat}), 137.5 (s, C_{quat}), 135.5 (d, $J_{C,P}$ = 12 Hz, CH_{Ar}), 134.4 (s, CH_{Ar}), 133.8 (d, $J_{C,P}$ = 11 Hz, CH_{Ar}), 130.0 (d, $J_{C,P}$ = 5 Hz, PCH_{Ar}), 129.2 (d, $J_{C,P}$ = 12 Hz, PCH_{Ar}), 127.6 (s, CH_{Ar}), 127.5 (s, CH_{Ar}), 127.2 (s, CH_{Ar}), 127.1 (s, CH_{Ar}), 123.1 (d, $^4J_{C,P}$ = 3 Hz, NCH=CHN), 121.4 (br s, NCH=CHN), 121.1 (s, CH_{Ar}), 111.0 (s, CH_{Ar}), 26.7 (br s, Ru–*C*H(Bcat)),# 21.2 (s, C_6MeH_2), 21.1 (s, C_6MeH_2), 20.0 (s, C_6MeH_2), 19.9 (s, C_6MeH_2), 16.2 (s, C_6MeH_2) ppm. #Assignment confirmed by ^{13}C–^{1}H HSQC. ^{11}B{^{1}H} NMR (128 MHz, C_6D_6, 298 K): δ = 43.0 (vbr s) ppm. Elemental analysis calcd (%) for $C_{63}H_{57}BN_2O_2P_2Ru$ [1047.94]: C, 72.20; H, 5.48; N, 2.67. Repeated attempts at analysis gave consistently low % C values. For example; Found: C, 71.49; H, 5.10; N, 2.54.

Reaction of 1 with B_2cat_2: [Ru(IMes)'$(PPh_3)_2$H] **1** (10 mg, 0.01 mmol) and B_2cat_2 (2.5 mg, 0.01 mol) were combined in C_6D_6 (0.5 mL) in a J. Youngs resealable NMR tube and the reaction monitored by ^{1}H and ^{31}P{^{1}H} NMR spectroscopy over ca. 1.5 h. Complex **5** was observed as the major ruthenium containing product of the reaction.

[Ru(IMes)"$(PPh_3)(CO)_2$] **6**: Addition of CO (1 atm) to a C_6D_6 solution (0.5 mL) of **2** (10 mg, 0.01 mmol) in a J. Youngs resealable NMR tube led to an instantaneous colour change from red to colourless due to the formation of **6**. The solution was concentrated and layered with hexane to give **6** as colourless crystals (5 mg, 64%). ^{1}H NMR (400 MHz, C_6D_6, 298 K): δ = 7.65–7.59 (m, 6H, Ar), 7.11 (m, 6H, Ar), 7.06–7.02 (m, 3H, Ar), 6.74 (s, 2H, Ar), 6.68 (br s, 2H, Ar), 6.58 (br s, 2H, Ar), 2.28-2.17 (m, 4H, $RuCH_2$), 2.16 (s, 6H, $C_6Me_2H_3$), 2.07 (s, 6H, $C_6Me_2H_3$) ppm. ^{31}P{^{1}H} NMR (162 MHz, C_6D_6, 298 K): δ = 46.1 (s) ppm. ^{13}C{^{1}H} DEPTQ NMR (101 MHz, C_6D_6, 298 K): δ = 197.7 (d, $^2J_{C,P}$ = 8 Hz, Ru–*C*O), 193.0 (d, $^2J_{C,P}$ = 92 Hz, Ru–C_{NHC}), 153.8 (s, C_{quat}), 136.7 (s, C_{quat}), 136.2 (d, $J_{C,P}$ = 18 Hz, PC_{quat}), 135.7 (s, C_{quat}), 134.1 (d, $J_{C,P}$ = 18 Hz, CH_{Ar}), 129.6 (s, CH_{Ar}), 129.3 (s, C_{quat}), 128.4 (d, $J_{C,P}$ = 9 Hz, PCH_{Ar}), 125.9 (s, CH_{Ar}), 124.4 (s, CH_{Ar}), 121.0 (d, $J_{C,P}$ = 2 Hz, NCH=NCH), 21.7 (d, $^2J_{C,P}$ = 9 Hz, Ru–CH_2), 21.3 (s, $C_6Me_2H_2$), 19.0 (s, $C_6Me_2H_2$) ppm. IR (ATR [cm^{-1}]): 1995 (s, ν_{CO}), 1930 (s, ν_{CO}). Elemental analysis calcd (%) for $C_{41}H_{37}N_2O_2Pru$ [721.78]: C, 68.22; H, 5.12; N, 3.88. Found: C, 68.28; H, 5.18; N, 3.80.

Crystallographic details: Data for **6** were collected on an Agilent Xcalibur diffractometer and Mo–Kα radiation, while those for **1, 2, 3** and **5** were obtained using an Agilent SuperNova instrument and a Cu–Kα source. All experiments were conducted at 150 K, solved using SHELXT[34] and refined using SHELXL[34,35] via the Olex2[36] interface.

Refinements were largely straightforward and only pertinent points of note will be detailed hereafter. The hydride was located and refined at a distance of 1.6 Å from the ruthenium centre in **1**. In **2**, the hydrogen atoms attached to C2 and C3 in the structure were readily located, and each was refined subject to being a distance of 0.98 Å from the relevant parent atom. The asymmetric unit in the structure of **3** was seen to comprise one molecule of the ruthenium complex and a diethyl ether moiety with half site occupancy. The latter lies close to a crystallographic inversion centre and is consequently disordered with itself. Solvent refinement was completed with the inclusion of distance and ADP restraints in order to help achieve a chemically sensible convergence. The crystal was twinned and the two main components were accounted for at the point of integration. A parallel integration that recognised a third component degraded the overall data set, probably because the third component did not contribute to the diffraction pattern at a very high level. As such, integration of components beyond the two major ones was abandoned and the optimal refinement is presented herein. In addition to one molecule of the ruthenium containing complex, the motif in **5** was found to include half of a molecule of benzene (disordered in a 75:25 ratio) proximate to a crystallographic inversion centre. Distance and ADP restraints were employed in this disordered region to assist convergence. The hydride ligand was readily located and, subsequently, refined without restraints.

Deposition Numbers 2219479 (for **2**), 2219480 (for **3**), 2219481 (for **1**), 2219482 (for **5**) and 2219483 (for **6**) contain the Supporting crystallographic data for this paper. These data are provided free of charge by the joint Cambridge Crystallographic Data Centre and Fachinformationszentrum Karlsruhe Access Structures service.

Acknowledgements

This work was supported by the EPSRC (grant EP/T019743/1 for AFP) and the European Union's Horizon 2020 research and innovation programme under the Marie Skłodowska-Curie grant agreement No 792674 (FMM). VVI thanks MINECO/FEDER (CTQ2017-83421-P) and Gobierno de Aragón (GA/FEDER, Inorganic Molecular Architecture Group E08_17R) for financial support and MINECO/FEDER for a FPI fellowship. We thank Dr David Liptrot for assistance with ATR-IR measurements and the anonymous reviewers for valuable experimental suggestions.

Research Article
doi.org/10.1002/ejic.202300037

Conflict of Interest

The authors declare no conflicts of interest.

Data Availability Statement

The data that support the findings of this study are available in the Supporting material for this article.

Keywords: carbene ligands · C–H activation · ruthenium · zinc

[1] a) W. A. Herrmann, C. Köcher, *Angew. Chem. Int. Ed.* **1997**, *36*, 2162–2187; *Angew. Chem.* **1997**, *109*, 2256–2282; b) T. Weskamp, V. P. W. Böhm, W. A. Herrmann, *J. Organomet. Chem.* **2000**, *600*, 12–22; c) W. A. Herrmann, *Angew. Chem. Int. Ed.* **2002**, *41*, 1290–1309; *Angew. Chem.* **2002**, *114*, 1342–1363; d) *N-Heterocyclic Carbenes in Synthesis* (Ed.: S. P. Nolan), Wiley-VCH, Weinheim, **2006**; e) F. E. Hahn, M. C. Jahnke, *Angew. Chem. Int. Ed.* **2008**, *47*, 3122–3172; *Angew. Chem.* **2008**, *120*, 3166–3216; f) S. Díez-González, N. Marion, S. P. Nolan, *Chem. Rev.* **2009**, *109*, 3612–3676; g) *N-Heterocyclic Carbenes* (Ed.: S. Díez-González), Royal Society of Chemistry, Cambridge, **2011**; h) *N-Heterocyclic Carbenes in Transition Metal Catalysis and Organocatalysis* (Ed.: C. S. J. Cazin), Springer, Dordrecht, **2011**.

[2] Y. H. Lee, B. Morandi, *Coord. Chem. Rev.* **2019**, *386*, 96–118.

[3] M. N. Hopkinson, C. Richter, M. Schedler, F. Glorius, *Nature* **2014**, *510*, 485–496.

[4] a) C. M. Crudden, D. P. Allen, *Coord. Chem. Rev.* **2004**, *248*, 2247–2273; b) T. P. Nicholls, J. R. Williams, C. E. Willans, in *Adv. Organomet. Chem., Vol. 75*, (Ed.: P. J. Perez), **2021**, 245–329.

[5] Q. Zhao, G. R. Meng, S. P. Nolan, M. Szostak, *Chem. Rev.* **2020**, *120*, 1981–2048.

[6] a) S. H. Hong, A. G. Wenzel, T. T. Salguero, M. W. Day, R. H. Grubbs, *J. Am. Chem. Soc.* **2007**, *129*, 7961–7968; b) E. M. Leitao, S. R. Dubberley, W. E. Piers, Q. Wu, R. McDonald, *Chem. Eur. J.* **2008**, *14*, 11565–11572; c) L. Vieille-Petit, X. J. Luan, M. Gatti, S. Blumentritt, A. Linden, H. Clavier, S. P. Nolan, R. Dorta, *Chem. Commun.* **2009**, 3783–3785.

[7] For a recent review, see: a) C. S. Tiwari, P. M. Illam, S. N. R. Donthireddy, A. Rit, *Chem. Eur. J.* **2021**, *27*, 16581–16600. For specific examples, see: b) S. Burling, B. M. Paine, D. Nama, V. S. Brown, M. F. Mahon, T. J. Prior, P. S. Pregosin, M. K. Whittlesey, J. M. J. Williams, *J. Am. Chem. Soc.* **2007**, *129*, 1987–1995; c) K. Endo, R. H. Grubbs, *J. Am. Chem. Soc.* **2011**, *133*, 8525–8527; d) D. Paul, B. Beiring, M. Plois, N. Ortega, S. Kock, D. Schlüns, J. Neugebauer, R. Wolf, F. Glorius, *Organometallics* **2016**, *35*, 3641–3646; e) Q. Chen, Q. Liu, J. Xiao, X. B. Leng, L. Deng, *J. Am. Chem. Soc.* **2021**, *143*, 19956–19965; f) Y. Xu, Q. Gan, A. E. Samkian, J. H. Ko, R. H. Grubbs, *Angew. Chem. Int. Ed.* **2022**, *61*, e202113089; *Angew. Chem.* **2022**, *134*, e202113089; g) A. Hamza, D. Moock, C. Schlepphorst, J. Schneidewind, W. Baumann, F. Glorius, *Chem. Sci.* **2022**, *13*, 985–995.

[8] M. Espinal-Viguri, V. Varela-Izquierdo, F. M. Miloserdov, I. M. Riddlestone, M. F. Mahon, M. K. Whittlesey, *Dalton Trans.* **2019**, *48*, 4176–4189.

[9] a) J. K. Huang, E. D. Stevens, S. P. Nolan, *Organometallics* **2000**, *19*, 1194–1197; b) M. J. Chilvers, R. F. R. Jazzar, M. F. Mahon, M. K. Whittlesey, *Adv. Synth. Catal.* **2003**, *345*, 1111–1114; c) N. M. Scott, V. Pons, E. D. Stevens, D. M. Heinekey, S. P. Nolan, *Angew. Chem. Int. Ed.* **2005**, *44*, 2512–2515; *Angew. Chem.* **2005**, *117*, 2568–2571.

[10] F. M. Miloserdov, N. A. Rajabi, J. P. Lowe, M. F. Mahon, S. A. Macgregor, M. K. Whittlesey, *J. Am. Chem. Soc.* **2020**, *142*, 6340–6349.

[11] K. Abdur-Rashid, T. Fedorkiw, A. J. Lough, R. H. Morris, *Organometallics* **2004**, *23*, 86–94.

[12] J. M. Blacquiere, C. S. Higman, S. I. Gorelsky, N. J. Beach, S. J. Dalgarno, D. E. Fogg, *Angew. Chem. Int. Ed.* **2011**, *50*, 916–919; *Angew. Chem.* **2011**, *123*, 946–949.

[13] a) S. Burling, G. Kociok-Kohn, M. F. Mahon, M. K. Whittlesey, J. M. J. Williams, *Organometallics* **2005**, *24*, 5868–5878; b) S. Burling, L. J. L. Häller, E. Mas-Marzá, A. Moreno, S. A. Macgregor, M. F. Mahon, P. S. Pregosin, M. K. Whittlesey, *Chem. Eur. J.* **2009**, *15*, 10912–10923; c) C. L. Lund, M. J. Sgro, R. Cariou, D. W. Stephan, *Organometallics* **2012**, *31*, 802–805; d) T. E. Wang, C. Pranckevicius, C. L. Lund, M. J. Sgro, D. W. Stephan, *Organometallics* **2013**, *32*, 2168–2177.

[14] A useful comparison is provided by a report of the isolation of 14-electron $[Ru(P^iPr_3)_2HCl]$, which was subsequently shown to be the dinitrogen adduct, $[Ru(P^iPr_3)_2(N_2)HCl]$. P. A. van der Schaaf, R. Kolly, A. Hafner, *Chem. Commun.* **2000**, 1045–1047.

[15] Note that the same $[Ru(P^iPr_3)_2HCl]$ species from Ref. [14] was reported to exist as a dimer with bridging chloride ligands (J. N. Coalter III, J. C. Huffman, W. E. Streib, K. G. Caulton, *Inorg. Chem.* **2000**, *39*, 3757–3764). With the data available to us, we cannot rule out the singlet arising from a dimeric species.

[16] Changing the solvent from THF to CH_2Cl_2 resulted only in decomposition.

[17] a) G. Schnee, C. Fliedel, T. Aviles, S. Dagorne, *Eur. J. Inorg. Chem.* **2013**, 3699–3709; b) A. Rit, T. P. Spaniol, L. Maron, J. Okuda, *Organometallics* **2014**, *33*, 2039–2047.

[18] a) J. Navarro, O. Torres, M. Martín, E. Sola, *J. Am. Chem. Soc.* **2011**, *133*, 9738–9740; b) C. Y. Tang, N. Phillips, M. J. Kelly, S. Aldridge, *Chem. Commun.* **2012**, *48*, 11999–12001; c) H. J. Liu, M. S. Ziegler, T. D. Tilley, *Polyhedron* **2014**, *84*, 203–208; d) H. J. Liu, M. S. Ziegler, T. D. Tilley, *Dalton Trans.* **2018**, *47*, 12138–12146.

[19] For examples of double N-aryl activation see: a) N. Stylianides, A. A. Danopoulos, D. Pugh, F. Hancock, A. Zanotti-Gerosa, *Organometallics* **2007**, *26*, 5627–5635; b) B. Eguillor, M. A. Esteruelas, V. Lezaun, M. Olivan, E. Onate, J. Y. Tsai, C. J. Xia, *Chem. Eur. J.* **2016**, *22*, 9106–9110; c) Z.-B. Yan, K.-L. Dai, B.-M. Yang, Z.-H. Li, Y.-Q. Tu, F.-M. Zhang, X.-M. Zhang, M. Peng, Q.-L. Chen, Z.-R. Jing, *Sci. China Chem.* **2020**, *63*, 1761–1766; d) K. Nakanishi, J. O. C. Jimenez-Halla, S. Yamazoe, M. Nakamoto, R. Shang, Y. Yamamoto, *Inorg. Chem.* **2021**, *60*, 9970–9976.

[20] B. Cordero, V. Gómez, A. E. Platero-Prats, M. Revés, J. Echeverría, E. Cremades, F. Barragán, S. Alvarez, *Dalton Trans.* **2008**, 2832–2838.

[21] a) I. M. Riddlestone, N. A. Rajabi, J. P. Lowe, M. F. Mahon, S. A. Macgregor, M. K. Whittlesey, *J. Am. Chem. Soc.* **2016**, *138*, 11081–11084; b) N. O'Leary, F. M. Miloserdov, M. F. Mahon, M. K. Whittlesey, *Dalton Trans.* **2019**, *48*, 14000–14009; c) F. M. Miloserdov, A.-F. Pécharman, L. Sotorrios, N. A. Rajabi, J. P. Lowe, S. A. Macgregor, M. F. Mahon, M. K. Whittlesey, *Inorg. Chem.* **2021**, *60*, 16256–16265; d) L. Sotorrios, F. M. Miloserdov, A.-F. Pécharman, J. P. Lowe, S. A. Macgregor, M. F. Mahon, M. K. Whittlesey, *Angew. Chem. Int. Ed.* **2022**, *61*, e202117495; *Angew. Chem.* **2022**, *134*, e202117495.

[22] A VT NMR study of the **1** in $C_6D_5CD_3$ showed no broadening of the hydride resonance at 213 K when the sample was under argon (Figure S16). However, when the Ar atmosphere was replaced by H_2 and the sample inserted back into the pre-cooled spectrometer at 213 K, noticeable broadening of the signal was apparent, although to a lesser extent than when H_2 was introduced and the sample cooled down to low temperature from room temperature inside the NMR spectrometer (Figure S12). This we attribute to some association of **1** with H_2, which impacts more on the appearance of the Ru–H signal when dihydrogen is present for a longer time before cooling to low temperature.

[23] The more forcing conditions required for the formation of the IMes complex **1** as opposed to SIMes derivative $[Ru(SIMes)'(PPh_3)_2H]$ (see Ref. [11]) is in line with the proposal by Fogg and co-workers of an 'inverse trans effect' for unsaturated NHCs, whereby they can inhibit dissociation of a ligand (such as a phosphine) in a trans position. J. A. M. Lummiss, C. S. Higman, D. L. Fyson, R. McDonald, D. E. Fogg, *Chem. Sci.* **2015**, *6*, 6739–6746.

[24] Interestingly, heating for this amount of time led to the direct formation of small amounts (10% isolated yield) of **2**.

[25] For more discussion of structural distortions in **1** relative to **2**, **3**, **5** and **6**, see the Supporting Information.

[26] a) A. F. Borowski, B. Donnadieu, J. C. Daran, S. Sabo-Etienne, B. Chaudret, *Chem. Commun.* **2000**, 543–544; b) D. Giunta, M. Hölscher, C. W. Lehmann, R. Mynott, C. Wirtz, W. Leitner, *Adv. Synth. Catal.* **2003**, *345*, 1139–1145.

[27] a) P. Ríos, R. Martín-de la Calle, P. Vidossich, F. J. Fernández-de-Córdova, A. Lledós, S. Conejero, *Chem. Sci.* **2021**, *12*, 1647–1655; b) P. Ríos, F. J. Fernández-de-Córdova, J. Borge, N. Curado, A. Lledós, S. Conejero, *Eur. J. Inorg. Chem.* **2021**, 3528–3539.

[28] C. M. Kelly, J. T. Fuller III, C. M. Macaulay, R. McDonald, M. J. Ferguson, S. M. Bischof, O. L. Sydora, D. H. Ess, M. Stradiotto, L. Turculet, *Angew. Chem. Int. Ed.* **2017**, *56*, 6312–6316; *Angew. Chem.* **2017**, *129*, 6409–6413.

[29] $[Fe(IMes)'_2]$, $[Co(IMes)'_2]$ and $[Pt(IMes)(IMes)'][BAr^F_4]$ all react with silanes to undergo silylation of one of the arms of the carbene, which remain cyclometallated. a) Z. Ouyang, L. Deng, *Organometallics* **2013**, *32*, 7268–

7271; b) Z. Mo, Y. Liu, L. Deng, *Angew. Chem. Int. Ed.* **2013**, *52*, 10485–10489; *Angew. Chem.* **2013**, *125*, 11045–11049; c) P. Ríos, H. Fouilloux, J. Díez, P. Vidossich, A. Lledós, S. Conejero, *Chem. Eur. J.* **2019**, *25*, 11346–11355.

[30] The Ru–C_{ipso} distance in the Tilley complex is 2.420(9) Å. As the corresponding bond lengths in both **5** (2.586(3) Å) and **1** (2.6540(18) Å) are much longer, neither compound appears to exhibit a stabilising C_{ipso} interaction.

[31] a) R. N. Perutz, S. Sabo-Etienne, *Angew. Chem. Int. Ed.* **2007**, *46*, 2578–2592; *Angew. Chem.* **2007**, *119*, 2630–2645; b) R. N. Perutz, S. Sabo-Etienne, A. S. Weller, *Angew. Chem. Int. Ed.* **2022**, *61*, e202111462; *Angew. Chem.* **2022**, *134*, e202111462.

[32] R. A. Schunn, E. R. Wonchoba, G. Wilkinson, *Inorg. Synth.* **1972**, *13*, 131–134; Prior to use, we dried $[Ru(PPh_3)_3HCl]$·toluene under high vacuum and ground it to a fine powder affording a material with ca. 0.8 molecules of toluene per Ru based on ^{1}H NMR spectroscopy.

[33] X. Bantrei, S. P. Nolan, *Nat. Protoc.* **2011**, *6*, 69–77.

[34] G. M. Sheldrick, *Acta Crystallogr. Sect. C* **2015**, *C71*, 3–8.

[35] G. M. Sheldrick, *Acta Crystallogr., Sect. A: Found. Adv.* **2015**, *A71*, 3–8.

[36] O. V. Dolomanov, L. J. Bourhis, R. J. Gildea, J. A. K. Howard, H. Puschmann, *J. Appl. Crystallogr.* **2009**, *42*, 339–341.

Manuscript received: January 20, 2023
Revised manuscript received: February 16, 2023
Accepted manuscript online: February 17, 2023

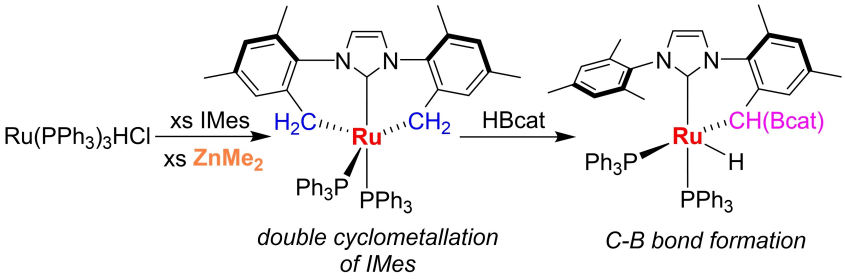

Dr. A.-F. M. Pécharman, E. M. Roberts, Dr. F. M. Miloserdov, Dr. V. Varela-Izquierdo, Dr. M. F. Mahon, Prof. M. K. Whittlesey**

1 – 11

Isolation of Bis- and Mono-Cyclometallated Ru–IMes Complexes upon Reaction of [Ru(PPh$_3$)$_3$HCl], IMes and ZnMe$_2$

Addition of ZnMe$_2$ to a mixture of [Ru(PPh$_3$)$_3$HCl] and IMes affords the doubly cyclometallated Ru–NHC complex [Ru(IMes)"(PPh$_3$)$_2$], which undergoes hydrogenation with H$_2$, PhSiH$_3$ and HBpin, but borylation of a metallated arm with HBcat.